RESEARCH ARTICLE

Cortical and thalamic inputs exert cell type-specific feedforward inhibition on striatal GABAergic interneurons

Maxime Assous 🆔 | James M. Tepper 🆔

Center for Molecular and Behavioral Neuroscience, Rutgers University, Newark, New Jersey

Correspondence
Maxime Assous and James M. Tepper, Center for Molecular and Behavioral Neuroscience, Rutgers University, Newark, NJ 07102.
Email: maxime.assous@newark.rutgers.edu (M. A.) and jtepper@newark.rutgers.edu (J. M. T.)

Abstract

The classical view of striatal GABAergic interneuron function has been that they operate as largely independent, parallel, feedforward inhibitory elements providing inhibitory inputs to spiny projection neurons (SPNs). Much recent evidence has shown that the extrinsic innervation of striatal interneurons is not indiscriminate but rather very specific, and that striatal interneurons are themselves interconnected in a cell type-specific manner. This suggests that the ultimate effect of extrinsic inputs on striatal neuronal activity depends critically on synaptic interactions within interneuronal circuitry. Here, we compared the cortical and thalamic input to two recently described subtypes of striatal GABAergic interneurons, tyrosine hydroxylase-expressing interneurons (THINs), and spontaneously active bursty interneurons (SABIs) using transgenic TH-Cre and Htr3a-Cre mice of both sexes. Our results show that both THINs and SABIs receive strong excitatory input from the motor cortex and the thalamic parafascicular nucleus. Cortical optogenetic stimulation also evokes disynaptic inhibitory GABAergic responses in THINs but not in SABIs. In contrast, optogenetic stimulation of the parafascicular nucleus induces disynaptic inhibitory responses in both interneuron populations. However, the short-term plasticity of these disynaptic inhibitory responses is different suggesting the involvement of different intrastriatal microcircuits. Altogether, our results point to highly specific interneuronal circuits that are selectively engaged by different excitatory inputs.

KEYWORDS
feedforward inhibition, GABAergic interneurons, glutamate, striatum

1 | INTRODUCTION
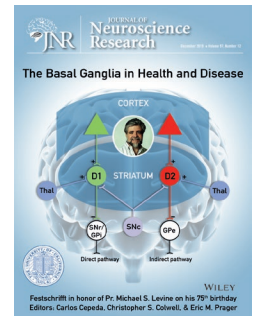
The striatum constitutes the main input structure of the basal ganglia. Its major excitatory projections arise from multiple regions of the cerebral cortex and several thalamic nuclei (Buchwald et al., 1973; Kemp & Powell, 1971; Smith, Raju, Pare, & Sidibe, 2004). One of the main functions attributed to the striatum is the integration of these excitatory inputs and transfer of this information to downstream basal ganglia nuclei. Essentially, all regions of the cortex project to the striatum (Flaherty & Graybiel, 1993; Haber, 2016; Haber, Kim, Mailly, & Calzavara, 2006; Hintiryan et al., 2016; Yeterian & Van Hoesen, 1978) in a highly topographic manner (Alexander, DeLong, & Strick, 1986; Hintiryan et al., 2016; Mathai & Smith, 2011). Thalamostriatal projections originate principally from the intralaminar nuclei, specifically the centromedian/parafascicular complex or parafascicular nucleus (PfN) in rodents (Berendse & Groenewegen, 1990; Francois et al., 1991; McFarland & Haber, 2000; Sadikot,

Significance

We recently provided evidence that the innervation of striatal interneurons from cortex and thalamus shows great cell type specificity. Here, we demonstrate that two subtypes of striatal GABAergic interneurons, the THINs and the SABIs, show different polysynaptic responses following activation of either of these excitatory inputs. Differences in the short-term plasticities of the disynaptic inhibitory synaptic responses in THINs and SABIs to cortical or thalamic stimulation suggest that the inhibition is mediated through different GABAergic neurons. Understanding these intrastriatal interneuronal connections is fundamental to comprehend the functional integration of different extrinsic inputs to the striatum.

Parent, Smith, & Bolam, 1992; Smith et al., 2014, 2004; Smith & Parent, 1986). Thalamostriatal projections originating from the PfN are also topographically organized (Mandelbaum et al., 2019).

Cortical and thalamic inputs target both the spiny projection neurons (SPNs) as well as most striatal interneurons. It is notable that the innervation by these extrinsic sources shows different short-term plasticities suggesting that they may carry out different functions (Ding, Guzman, Peterson, Goldberg, & Surmeier, 2010; Ding, Peterson, & Surmeier, 2008; Ellender, Harwood, Kosillo, Capogna, & Bolam, 2013; Sciamanna, Ponterio, Mandolesi, Bonsi, & Pisani, 2015). As a general rule, the same afferent fibers make stronger excitatory connections onto interneurons than onto principal cells in striatum and elsewhere, leading to the idea that interneurons acutely shape network activity via feedforward inhibition (Cruikshank, Lewis, & Connors, 2007; Gabernet, Jadhav, Feldman, Carandini, & Scanziani, 2005; Isaacson & Scanziani, 2011; Mallet, Moine, Charpier, & Gonon, 2005; Parthasarathy & Graybiel, 1997; Ramanathan, Hanley, Deniau, & Bolam, 2002).

The classical view of striatal GABAergic interneuron function has been that they receive nonspecialized excitatory extrinsic inputs and provide feedforward inhibition to SPNs thereby regulating their spike-timing (Gittis & Kreitzer, 2012; Koós, Tepper, & Wilson, 2004). However, we recently showed that excitatory input, in particular from the PfN, is not homogeneous among interneurons but is instead very cell type specific. In particular, we showed that the typical response of neuropeptide Y-expressing low-threshold spike interneurons (LTSIs) to optogenetic thalamic stimulation is not a monosynaptic EPSP/C but rather a disynaptic inhibition, at least part of which comes from thalamic monosynaptic activation of tyrosine hydroxylase-expressing interneurons (THINs) (Assous et al., 2017; Assous & Tepper, 2018). Furthermore, we showed that striatal GABAergic and cholinergic interneurons form an interconnected network and that the impact of extrinsic inputs to the striatum depends critically on the intrastriatal microcircuitry (Assous et al., 2017; Assous & Tepper, 2018). As an example, we recently

identified and characterized a novel population of GABAergic interneurons that are transduced in Htr3a-Cre transgenic mice, spontaneously active bursty interneurons (SABIs). SABIs do not significantly synapse onto SPNs and seem to be the first example of an interneuron selective interneuron in the striatum (Assous et al., 2018; Tepper et al., 2018). Understanding how extrinsic inputs are processed by the intrinsic striatal circuitry is essential to understand how these inputs ultimately affect the SPNs and downstream basal ganglia structures. Here, we compare cortical and thalamic inputs to two populations of striatal GABAergic interneurons, the THINs and the SABIs. Using ex vivo brain slice recordings combined with optogenetic stimulation of thalamostriatal or corticostriatal terminals, we demonstrate that THINs and SABIs receive strong monosynaptic innervation from these extrinsic glutamatergic striatal input structures. In addition, we show that activation of these inputs elicits distinct inhibitory polysynaptic responses in these striatal interneurons.

2 | METHODS

2.1 | Animals

All procedures used in this study were performed in agreement with the National Institutes of Health Guide to the Care and Use of Laboratory Animals and with the approval of the Rutgers University-Newark Institutional Animal Care and Use Committee. Adult (3–8 months of age when slices were obtained) transgenic mice of both sexes (Htr3a-Cre (Tg(Htr3a-Cre) NO152Gsat/ Mmucd, UC Davis) (Gerfen, Paletzki, & Heintz, 2013), NPY-GFP (stock 006,417; The Jackson Laboratory), and TH-Cre [Tg(TH–Cre)12Gsat; Gene Expression Nervous System Atlas [GENSAT]) were generated and maintained as hemizygotic. Mice were housed in groups of up to four per cage and maintained on a 12-hr light cycle (07:00 a.m.–07:00 p.m.) with ad libitum access to food and water.

2.2 | Intracerebral viral injection

A non-competent Adeno-associated virus (AAV5-CAMKIIa-hChR2(H134R)-EYFP, Penn Vector Core, AV-5-26969P, t ≥ 10^{13} vg/ml, Addgene 26969P) was injected into the PfN or motor cortex to study the thalamic and cortical input to THINs and SABIs (targeted in Htr3a-Cre mice). In addition, an AAV5-CAG-Flex-tdTomato virus (University of North Carolina, Vector Core Services, Chapel Hill, NC, t ≥ 10^{13} vg/ml, Addgene 28306) was injected into the striatum of TH-Cre and Htr3a-Cre mice.

The surgery and viral injections took place inside a Biosafety Level-2 isolation hood as previously described (Assous et al., 2017). Htr3a-Cre and TH-Cre mice were anesthetized with isoflurane (1.5%–2.5%, delivered with O_2, 1 ml/min) and placed within a stereotaxic frame. Bupivacaine was used as a local anesthetic at the site of the surgery. Coordinates to target the PfN of the thalamus were −2.3 mm anteroposterior and 0.75 mm lateral to

Bregma. 0.2 µl of virus was delivered by glass pipette using a Nanoject II (Drummond) to two sites in each mouse (total 400 nl): −3.2 mm and −3.45 mm ventral to the brain surface to transduce as much of the PfN as possible. We have previously demonstrated that such injections are largely restricted to the boundaries of the PfN (Assous et al., 2017 and see Figure 1c,d). Possible contamination to neighboring thalamic nuclei was assessed after resectioning the thalamus and we excluded mice where the injection was not largely or completely restricted to the PfN. Although we cannot completely rule out the possibility of minor contamination by neighboring thalamic nuclei, such afferents could only comprise a tiny fraction of the transduced thalamostriatal inputs in our mice. Coordinates to target the striatum were 0.6 mm anteroposterior and 1.8 mm lateral to Bregma. Virus was delivered to three sites in each mouse: −2.25, −2.65 and −3.2 mm ventral to brain surface for a total volume of 1 µl. To target the motor cortex virus was injected to two sites in each mouse: 0.98 mm anterior 1.05 mm and 1.55 mm lateral to bregma and 0.75 mm ventral to brain surface for a total volume of 1 µl. Virus was injected at 9.2 nl/5 s (for cortical and striatal injections) or 4.6 nl/ 5 s (for thalamic injections), after which the pipette was left in place for 10 min before being slowly retracted. Mice survived for 4–6 weeks for expression of the viral transgene before being sacrificed.

2.3 | Imaging

Mice were deeply anesthetized with an intraperitoneal injection of 80 mg/kg ketamine/20 mg/kg xylazine. Brain tissue was fixed by
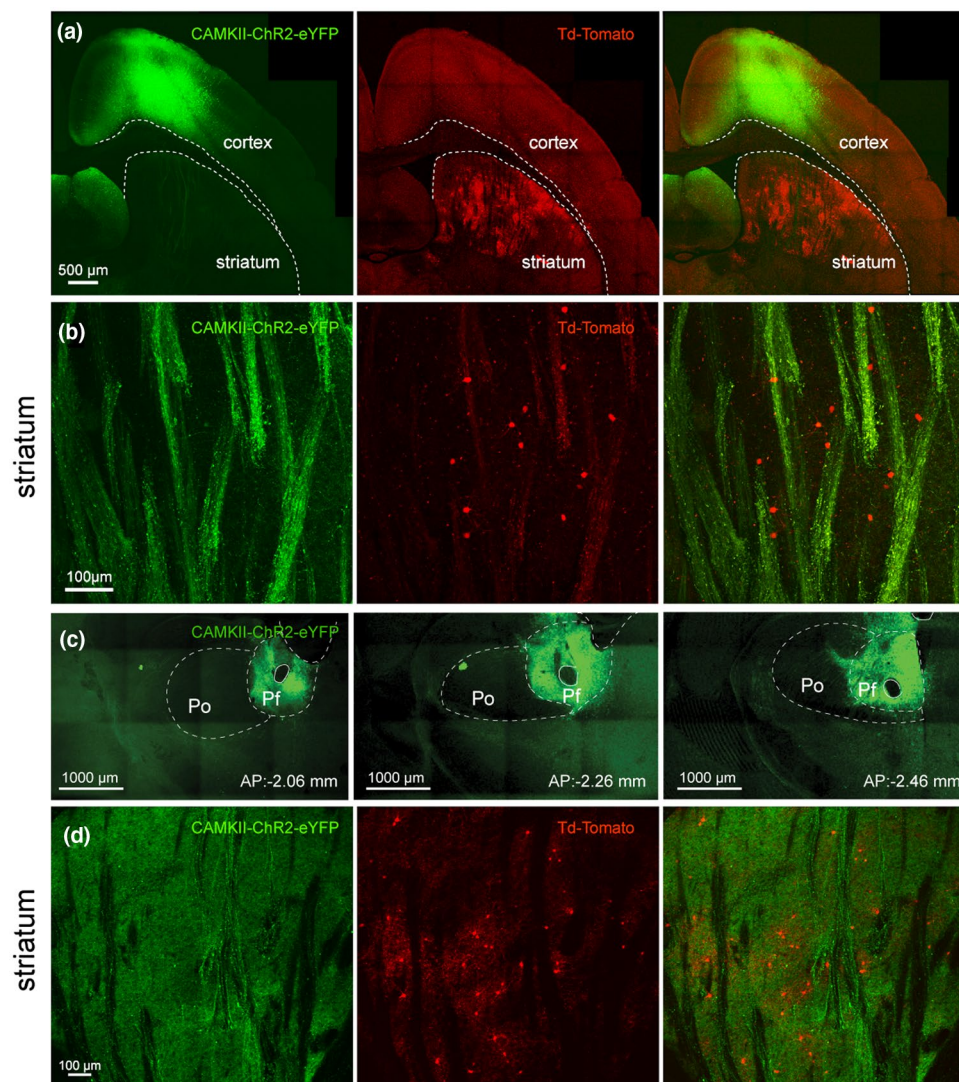
FIGURE 1 Cortical and thalamic innervation of striatal interneurons. (a) Confocal image of cortical neurons transfected with a CAMKII-ChR2-EYFP Adeno-associated virus (AAV, green) and Htr3a-Cre-transduced interneurons following striatal AAV-Flex-tdTomato injection (red) in a Htr3a transgenic mouse (oblique parahorizontal plane). (b) Higher magnification confocal image showing corticostriatal fibers in green and Htr3a-Cre-transduced interneurons in red. (c) Confocal image of the AAV-CAMKII-ChR2-EYFP injection site in the PfN at 3 anteroposterior anatomical levels (−206, −2.26 and −2.46 from bregma). (d) Confocal image of Htr3a-Cre transduced interneurons (red) and thalamostriatal axons (green, coronal section)

transcardial perfusion of 10 ml of ice-cold artificial cerebrospinal fluid (adjusted to 7.2–7.4 pH), followed by perfusion of 90–100 ml of 4% paraformaldehyde, 15% picric acid in phosphate buffer. Fixed brains were extracted and postfixed overnight in the perfusion fixative. 50–60 μm coronal or oblique parahorizontal sections were cut on a Vibratome 3000. Sections were mounted in Vectashield (Vector Labs, Burlingame, CA) and representative photomicrographs were taken at 10 and 60x using a confocal microscope (Fluoview FV1000, Olympus). Comparable pictures were taken using the same laser settings.

2.4 | Slice preparation and visualized in vitro whole-cell recording

Procedures were as described previously (Assous et al., 2017). Mice were deeply anesthetized with an intraperitoneal injection of 80 mg/kg ketamine/20 mg/kg xylazine 4–6 weeks after virus injection, and perfused transcardially with an ice cold N-methyl D-glucamine (NMDG) solution containing (in mM): 103.0 NMDG, 2.5 KCl, 1.2 NaH_2PO4, 30.0 $NaHCO_3$, 20.0 HEPES, 10.0 glucose, 101.0 HCl, 10.0 $MgSO_4$, 2.0 Thiourea, 3.0 sodium pyruvate, 12.0 N-acetyl cysteine, 0.5 $CaCl_2$ (saturated with 95% O2 and 5% CO2, pH 7.2–7.4). Mice were decapitated, and the brain was quickly removed into a beaker containing ice-cold oxygenated NMDG solution before slicing. Oblique 300-μm parahorizontal sections containing the striatum were cut in the same medium using a Vibratome 3000. Sections were immediately transferred to an oxygenated NMDG solution at 35°C for 5 min, after which they were transferred to oxygenated normal Ringer's solution at 25°C until used. The recording chamber was constantly perfused (2–4 ml/min) with oxygenated ACSF solution at 32–34°C. Drugs were applied in the perfusion medium and were dissolved freshly each day in Ringer's solution. Slices were initially visualized under epifluorescence illumination with a digital frame transfer camera (Cooke SensiCam) mounted on an Olympus BX50-WI epifluorescence upright microscope with a 40x long working distance water immersion lens to visualize the transfection field in the striatum. Visualization was then switched to infrared differential interference contrast microscopy for the actual patching of the neuron. Micropipettes for whole-cell recording were constructed from 1.2 mm outer diameter borosilicate pipettes on a Narishige PP-83 vertical puller. The standard internal solution for whole-cell current clamp recording was as follows (in mM): 130 K-gluconate, 10 KCl, 2 MgCl2, 10 HEPES, 4 Na2ATP, 0.4 Na2GTP, pH 7.3. Recording pipettes had a DC impedance of 3–5 MΩ. Membrane currents and potentials were recorded using an Axoclamp 700B amplifier (Molecular Devices) and digitized at 20 kHz with a CED Micro 1401 Mk II and a PC running Signal, version 5 (Cambridge Electronic Design). Sweeps were run at 20-s intervals. We used bicuculline methiodide (10 μM, Sigma) to block $GABA_A$ receptors and 6-Cyano-7-nitroquinoxaline-2,3-dione (CNQX, 10 μM, Tocris) and D-2-amino-5-phosphonovalerate (APV, 10 μM, Tocris) to block, respectively, AMPA and NMDA receptors.

2.5 | Experimental design and statistics

A total of 11 TH-Cre mice were used for studying the thalamic input to THINs (n = 28 THINs recorded) and 5 TH-Cre mice for the cortical input to these cells (n = 23 THINs recorded). Regarding the Htr3a-Cre mice, 11 mice were used for thalamic inputs (n = 25 SABIs recorded) and 4 for cortical inputs (n = 16 SABIs recorded). Most whole-cell recordings were analyzed using Signal (CED) and statistical analyses were performed using Prism (Graphpad). Statistical tests used were paired or unpaired two-tailed t-tests and exact p and t values are reported in the text. Box plots show the minimum and maximum interquartile ranges, and the mean and median value of the parameter.

3 | RESULTS

3.1 | Cortical input to THINs and SABIs

We previously demonstrated that THINs respond with short latency excitation to electrical stimulation of cortex (Ibáñez-Sandoval et al., 2010) suggesting a monosynaptic cortical innervation of THINs. Here, we examined in more detail the corticostriatal synaptic responses to the THINs including short-term synaptic plasticity as well as potential polysynaptic responses evoked by optogenetic stimulation of motor cortical areas. A CAMKII-ChR2 Adeno-Associated virus (AAV) was injected into the motor cortex (comprising M1 and M2) of TH-Cre mice (see methods) and a Flex-tdTomato AAV was injected into the dorsal striatum to visualize striatal THINs (Figures 1a,b and 2a). The vast majority of the recorded THINs in the dorsal striatum exhibited the typical intrinsic electrophysiological characteristics of the Type I THINs including a high-input resistance, averaging 750 MΩ (about an order of magnitude greater than SPNs or fast-spiking interneurons (FSIs), the presence of a prolonged plateau potential after injection of a depolarizing pulse and extreme spike frequency accommodation leading to depolarization block during modest depolarizing current injections in whole-cell recordings (Figure 2b; Assous et al., 2018; Ibáñez-Sandoval et al., 2010; Xenias, Ibanez-Sandoval, Koós, & Tepper, 2015). In both cell-attached and whole-cell current clamp recordings, these THINs often exhibited spontaneous tonic firing activity as previously described (Assous et al., 2018; Ibáñez-Sandoval et al., 2010). Optogenetic stimulation of corticostriatal terminals induced action potential firing in the vast majority of recorded THINs (Figure 2b–d). When hyperpolarized to prevent action potential firing, the optogenetic stimulation evoked short latency EPSPs (Figure 2e; EPSP size 3.76 mV ± 0.72, n = 8; onset latency from start of light pulse = 6.08 ms ± 0.178, n = 8). In voltage clamp, the stimulation evoked short latency EPSCs (Figure 2f–i, Vh = −70 mV; EPSC size 113.2 ± 22.45 pA, n = 23; onset latency 5.43 ± 0.121 ms) that were blocked by glutamate receptor antagonists (CNQX and APV, 10 μM, control: 147.5 ± 33.25 pA; CNQX/APV: 10.28 ± 2.005 pA; t(9) = 4.36, p = 0.0018, two-tailed paired t-test, n = 10; Figure 2f,h).

We then examined the short-term plasticity of the glutamatergic corticostriatal synapses onto THINs by applying a train of
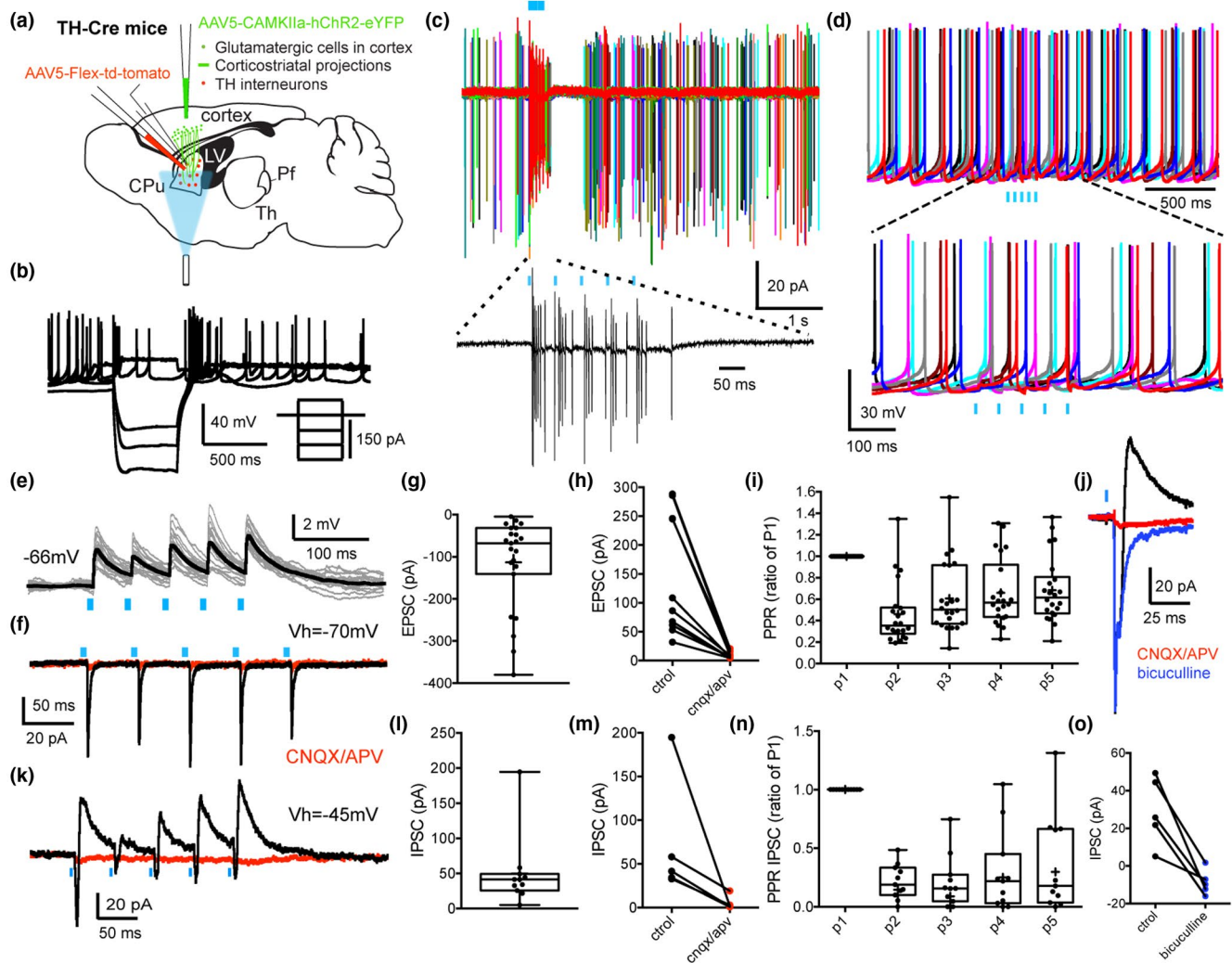
FIGURE 2 Cortical input to THINs. (a) Schematic illustrating the experimental preparation. (b) Typical responses to current injection in a Type I THIN in whole-cell recording. Note the spontaneous activity, the large input resistance and the depolarization inactivation after positive current injections. (c,d) Optogenetic stimulation of corticostriatal terminals evokes action potential firing in THINs both in cell-attached (c) and whole-cell current clamp modes (d). (e) Optogenetic stimulation evokes EPSPs (gray traces: individual trials, black trace: average) and EPSCs (f, Vh = −70 mV) blocked by CNQX/APV (10 μM, quantified in h). (g,l) Box plots quantifying the size of the EPSC and IPSC. (i) Histograms representing the short-term plasticity of the EPSCs (5 pulses, 20 Hz). (j,k) At a depolarized holding potential (Vh = −45 mV) optogenetic stimulation also evokes IPSCs (also blocked by CNQX/APV, and bicuculline10 μM, quantified in m and o). (n) Histograms representing the short-term plasticity of the IPSCs (5 pulses, 20 Hz). Box plots represent the minimum and maximum interquartile ranges, the mean and median. Blue bars in all figures indicate optical stimulation

five optical pulses (5 ms @ 20 Hz). Repetitive stimulation induced a depression in the synaptic response to the second optogenetic pulse followed by a partial recovery between the third and the fifth pulses ($p2_{ratio\ of\ p1}$: 0.461 ± 0.06; $p3_{ratio\ of\ p1}$: 0.607 ± 0.07; $p4_{ratio\ of\ p1}$: 0.659 ± 0.066; $p5_{ratio\ of\ p1}$: 0.683 ± 0.065, Figure 2i, n = 22). Interestingly, when the holding potential was changed to visualize IPSCs (Vh = −45 mV), we observed the concomitant presence of IPSCs following corticostriatal stimulation in 47.8% (n = 11/23 of recorded THINs, Figure 2j–o). The IPSC (amplitude: 49.94 ± 15.11 pA, Figure 2l) exhibited marked short-term depression (Figure 2n) and exhibited a significantly longer onset latency (9.02 ± 0.28 ms, n = 10) than the monosynaptic EPSC (see above,

$t(31) = 13.2$, $p < 0.0001$, unpaired t-test) suggesting the involvement of polysynaptic, most likely disynaptic, pathways. These IPSCs were blocked by bath application of CNQX and APV, 10 μM (control: 72.29 ± 30.93 pA vs. CNQX/APV, 10 μM: 5.14 ± 3.51, $t(4) = 2.135$, $p = 0.049$, two-tailed paired t-test, n = 5, Figure 2k,m) confirming the polysynaptic nature of these inhibitory responses. These IPSCs were also GABA$_A$ receptor dependent as they could be blocked with bicuculline (10 μM, n = 5, $t(4) = 4.8$, $p = 0.0087$ vs. control, two-tailed paired t-test, Figure 2o).

Using a similar strategy, we examined the cortical input to td-Tomato expressing SABIs recorded in the dorsal striatum targeted in the Htr3a-Cre mice (Assous et al., 2018; Figure 3a). In agreement
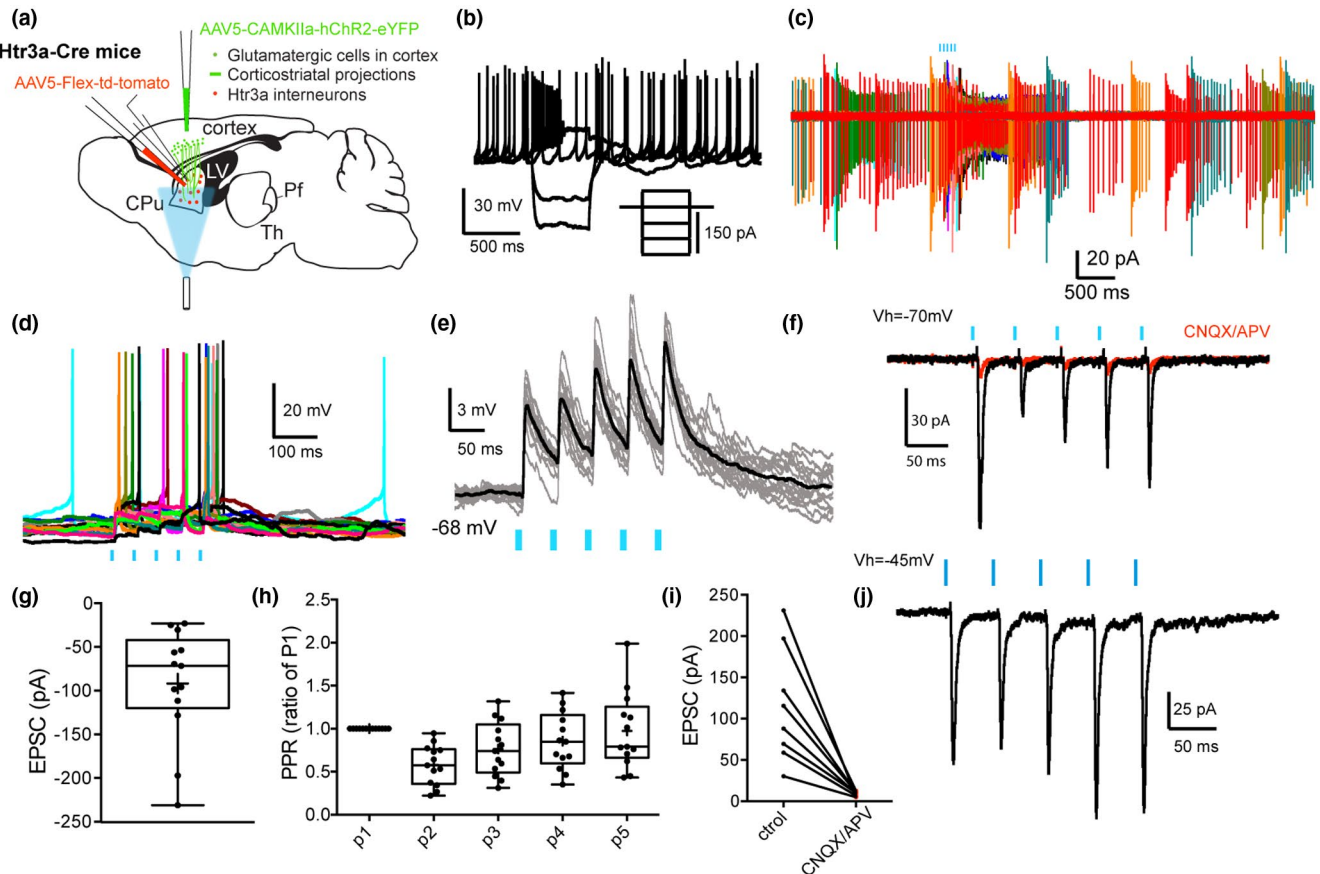
FIGURE 3 Cortical input to SABIs. (a) Experimental preparation. (b) Typical responses to current injection of a SABI in whole-cell recording. Note the spontaneous activity, the large input resistance and the depolarization inactivation after positive current injection. (c,d) Optogenetic stimulation of corticostriatal terminals evokes action potential firing in THINs recorded in cell-attached (c) and current clamp modes (d). Note the spontaneous bursting activity of the SABIs in the cell-attached recordings. (e) Optogenetic stimulation evokes EPSPs (gray traces: individual trials, black trace: average) and EPSCs (f, Vh = −70 mV) blocked by CNQX/APV (10 μM, quantified in i). (g) Box plot quantifying the size of the EPSC. (h) Histograms representing the short-term plasticity of the EPSCs (5 pulses, 20 Hz). (j) At depolarized holding potential (Vh = −45 mV) optogenetic stimulation does not evoke IPSCs but only EPSCs

with previous reports, we observed the presence of four different GABAergic interneuron subtypes targeted in the Htr3a-Cre mice (FSIs, neurogliaform interneurons [NGFIs], Fast-Adapting interneurons (FAIs) and SABIs; Assous et al., 2018; Faust et al., 2015, 2016). SABIs were identified based on their unique intrinsic electrophysiological properties including spontaneous activity (Figure 3b), high input resistance (>600 MΩ), spike frequency accommodation leading to depolarization block during modest depolarizing current injections, and especially their highly bursty firing pattern in cell-attached recordings (Figure 3c; Assous et al., 2018). Optogenetic stimulation of corticostriatal terminals induced burst firing in SABIs recorded in cell-attached voltage clamp mode (Figure 3c) as well as EPSPs and action potential firing in whole-cell current clamp recordings (Figure 3d,e). In voltage clamp, the stimulation evoked short latency EPSCs (Figure 3f–i, Vh = −70 mV; 91.67 ± 17.72 pA, n = 13; onset latency = 5.42 ± 0.1 ms) which were blocked by ionotropic glutamate receptor antagonists (CNQX and APV, 10 μM, control: 115.6 ± 24.55 pA; CNQX/APV: 8.83 ± 0.1 pA; t(7) = 4.39, p = 0.0032, two-tailed paired t-test, Figure 3f,i).

We then examined the short-term plasticity of the glutamatergic corticostriatal innervation of SABIs by applying a train of five optical pulses (5 ms @ 20 Hz). Repetitive stimulation induced short-term plasticity similar to that observed in THINs previously. There was a significant depression of the synaptic response to the second optogenetic pulse followed by a recovery between the third and the fifth pulses (p2$_{ratio of p1}$: 0.554 ± 0.123; p3$_{ratio of p1}$: 0.718 ± 0.149; p4$_{ratio of p1}$: 0.804 ± 0.169; p5$_{ratio of p1}$: 0.887 ± 0.183, n = 13, Figure 3h). In sharp contrast to THINs, however, when the holding voltage was changed to optimize visualization of IPSCs (Vh = −45 mV), IPSCs were never observed (Figure 3j).

3.2 | Thalamic input to THINs and SABIs

In a previous report, we demonstrated that THINs receive suprathreshold excitatory input from the PfN (Assous et al., 2017, Figure 4a–d). Here, we used a similar approach, by injecting AAV5-CAMKII-ChR2-eYFP into the PfN (Figure 1c,d). We confirmed that optogenetic stimulation of thalamostriatal terminals in virally
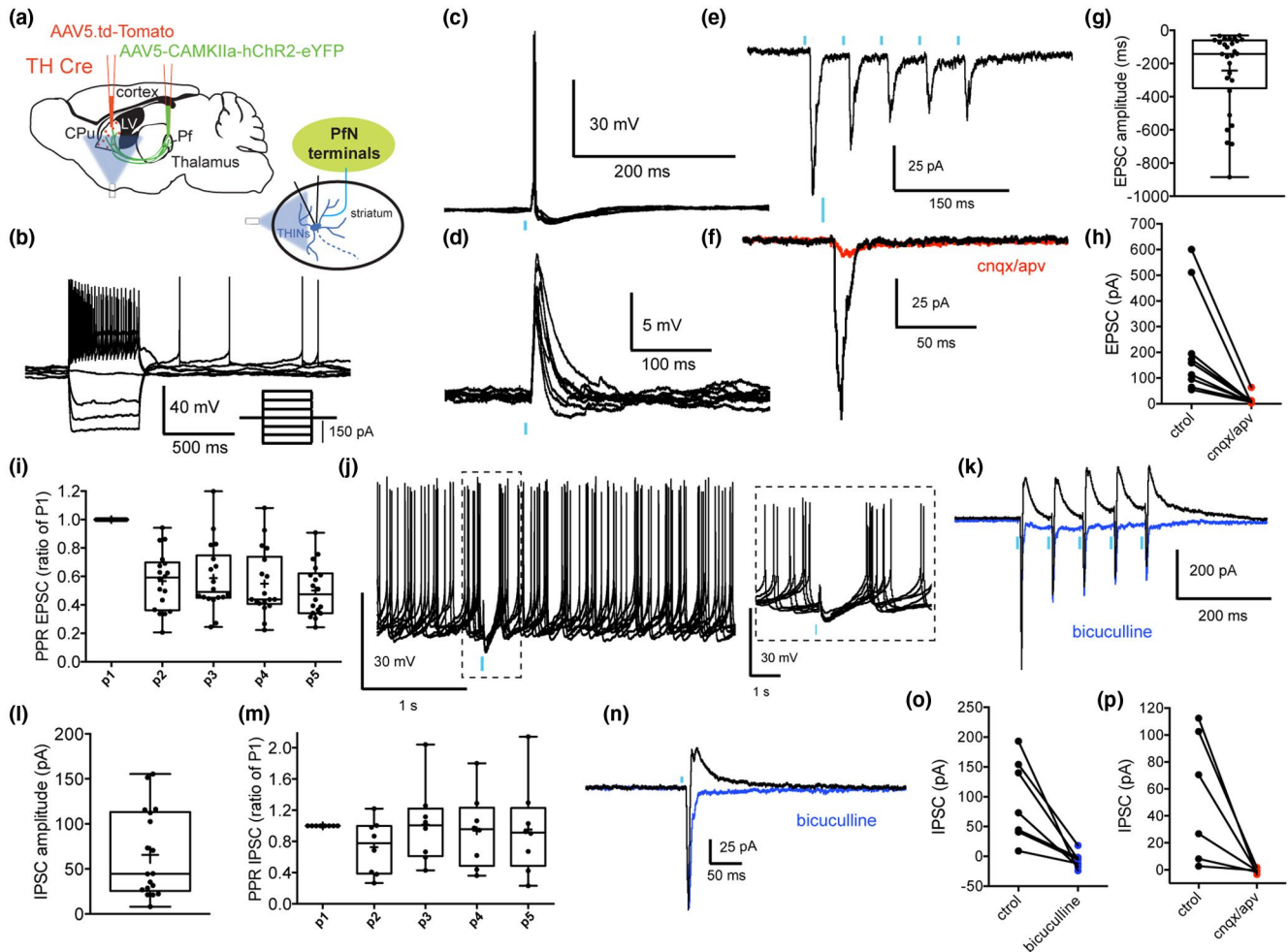
FIGURE 4 Thalamic input to THINs. (a) Experimental preparation. (b) Typical responses to current injection in a Type I THIN in whole-cell recording. (c) Optogenetic stimulation of thalamostriatal terminals evokes action potential firing in recorded THINs. (d,e) Optogenetic stimulation evokes EPSPs and EPSCs (Vh = −70 mV) blocked by CNQX/APV (10 μM, f). (g) Box plots of the amplitude of the EPSCs (g) induced by thalamic stimulation. (h) Quantification of the effect of bath application of glutamate receptor antagonists on the EPSC size (CNQX/APV, 10 μM). (i) Histograms representing the short-term plasticity of the EPSCs (5 pulses, 20 Hz). (j) Typical example of a spontaneously active THIN. Optogenetic stimulation (blue bar) evokes an EPSP-IPSP sequence (zoom in inset, right panel). (k,n) Optogenetic stimulation (Vh = −45 mV) evokes an IPSC that is blocked by bicuculline (10 μM, blue). (m) Histograms representing the short-term plasticity of the IPSCs (5 pulses, 20 Hz). (o) Quantification of the effect of bath application of bicuculline on the IPSC size (10 μM). (p) Quantification of the effect of bath application of glutamate receptor antagonists on the IPSC size (CNQX/APV, 10 μM)

transduced TH-Cre mice evoked short latency monosynaptic excitatory synaptic responses in electrophysiologically identified THINs (Figure 4c–h; EPSP size: 8.08 ± 0.96 mV, $n = 12$; EPSC size: 242.7 ± 45.7 pA, $n = 28$, that were blocked by glutamate receptor antagonists (CNQX/APV 10 μM). The EPSCs following train stimulation (5 pulses of 5 ms @ 20 Hz) showed short-term depression (p2$_{ratio of p1}$: 0.568 ± 0.048; p3$_{ratio of p1}$: 0.588 ± 0.057; p4$_{ratio of p1}$: 0.548 ± 0.055; p5$_{ratio of p1}$: 0.5 ± 0.04; Figure 4i). In addition, using techniques described above for optogenetic activation and recording of cortically evoked responses, we showed that the short latency glutamatergic EPSP/C was often followed by an IPSP/C ($n = 18/28$, 62.07%, Figure 4j–p). These IPSCs (65.67 ± 11.31 pA) exhibited a longer onset latency than that for the EPSC (8.797 ± 0.28 ms vs. 5.904 ± 0.16 ms for the EPSC, $t(40) = 9.43$, $p < 0.0001$, two-tailed

unpaired t-test) suggesting the involvement of polysynaptic, most likely disynaptic, pathways. This hypothesis was confirmed by blocking the IPSC/Ps by application of ionotropic glutamate receptor antagonists, CNQX/APV, 10 μM ($t(5) = 2.79$, $n = 6$, $p = 0.038$ vs. control, two-tailed paired t-test, Figure 4p). These IPSCs are also GABA$_A$ receptor dependent as they could also be blocked with bicuculline (10 μM, $n = 7$, $t(6) = 3.81$, two-tailed paired t-test, $p = 0.0089$ vs. control, Figure 4k,n,o). Unlike the EPSCs, the IPSCs exhibited no significant short-term plasticity after train stimulation (p2$_{ratio of p1}$: 0.727 ± 0.122; p3$_{ratio of p1}$: 1.015 ± 0.177; p4$_{ratio of p1}$: 0.937 ± 0.167; p5$_{ratio of p1}$: 0.952 ± 0.21; $n = 8$; Figure 4m).

Next, using a similar approach, we investigated the thalamic innervation of SABIs. AAV5-CAMKII-ChR2-eYFP virus was injected into the PfN of Htr3a-Cre mice and an AAV5-Floxed tdTomato

virus was injected into the striatum and tdTomato expressing SABIs were recorded from striatal slices (Figure 5a). Similar to PfN inputs to THINs, optogenetic stimulation of thalamostriatal fibers evoked EPSP/Cs and action potential firing in all recorded SABIs (Figure 5c–f; EPSP amplitude: 10.23 ± 1.3 mV, $n = 21$; EPSC amplitude: 227.6 ± 30.8 pA, $n = 23$). The EPSCs were glutamatergic as they were blocked by bath application of ionotropic glutamate receptor antagonists (CNQX/APV, 10 μM, $n = 6$, $t(5) = 3.07$, $p = 0.027$ vs. control, two-tailed paired t-test, Figure 5f,h,l). Similar to the thalamic evoked EPSCs in THINs, train stimulation of PfN axons elicited short-term depression in SABIs (5 pulses, 20 Hz; $p2_{ratio\ of\ p1}$: 0.7095 ± 0.098; $p3_{ratio\ of\ p1}$: 0.6716 ± 0.1067; $p4_{ratio\ of\ p1}$: 0.6433 ± 0.093; $p5_{ratio\ of\ p1}$: 0.6389 ± 0.098; Figure 5i). As with THINs, optogenetically elicited action potentials or EPSPs were often followed by an IPSP (Figure 5j). Similarly, voltage clamp recordings at −45 mV revealed the presence of IPSCs (Figure 5k–p). The occurrence of these IPSCs was more frequent than in THINs ($n = 21/25$ recorded SABIs, 84%, Figure 4m) and their amplitude was also significantly larger (151.5 ± 21.0 vs. 65.67 ± 11.31 pA; $t(37) = 3.43$ $p = 0.002$, two-tailed unpaired t-test).

The SABI IPSCs were mediated by GABA$_A$ receptors as they were blocked by bicuculline (10 μM; $t(7) = 3.96$, $p = 0.0055$ vs. control, two-tailed paired t-test, $n = 8$; Figure 5f,k,o) and also exhibited longer latencies (8.65 ± 0.55 ms) compared to the EPSC (4.99 ± 0.12, $t(37) = 7.02$, $p = 0.0001$, two-tailed unpaired t-test). The polysynaptic nature of the IPSCs was confirmed by their elimination with ionotropic glutamate receptor antagonists (CNQX/APV, 10 μM, $t(4) = 3.04$, $p = 0.038$ vs. control, two-tailed paired t-test, $n = 5$, Figure 5l,p). In contrast to the disynaptic IPSCs in THINs that exhibited no short-term plasticity, the IPSCs evoked in SABIs by optogenetic thalamic stimulation were depressing (5 pulses @ 20 Hz; $p2_{ratio\ of\ p1}$: 0.523 ± 0.097; $p3_{ratio\ of\ p1}$: 0.6 ± 0.101; $p4_{ratio\ of\ p1}$: 0.577 ± 0.074; $p5_{ratio\ of\ p1}$: 0.518 ± 0.011; $n = 10$; Figure 5n).

4 | DISCUSSION

Our results show that THINs and SABIs receive monosynaptic glutamatergic innervation from both cortex and thalamus. Cortical stimulation also evokes disynaptic IPSP/Cs selectively in THINs but
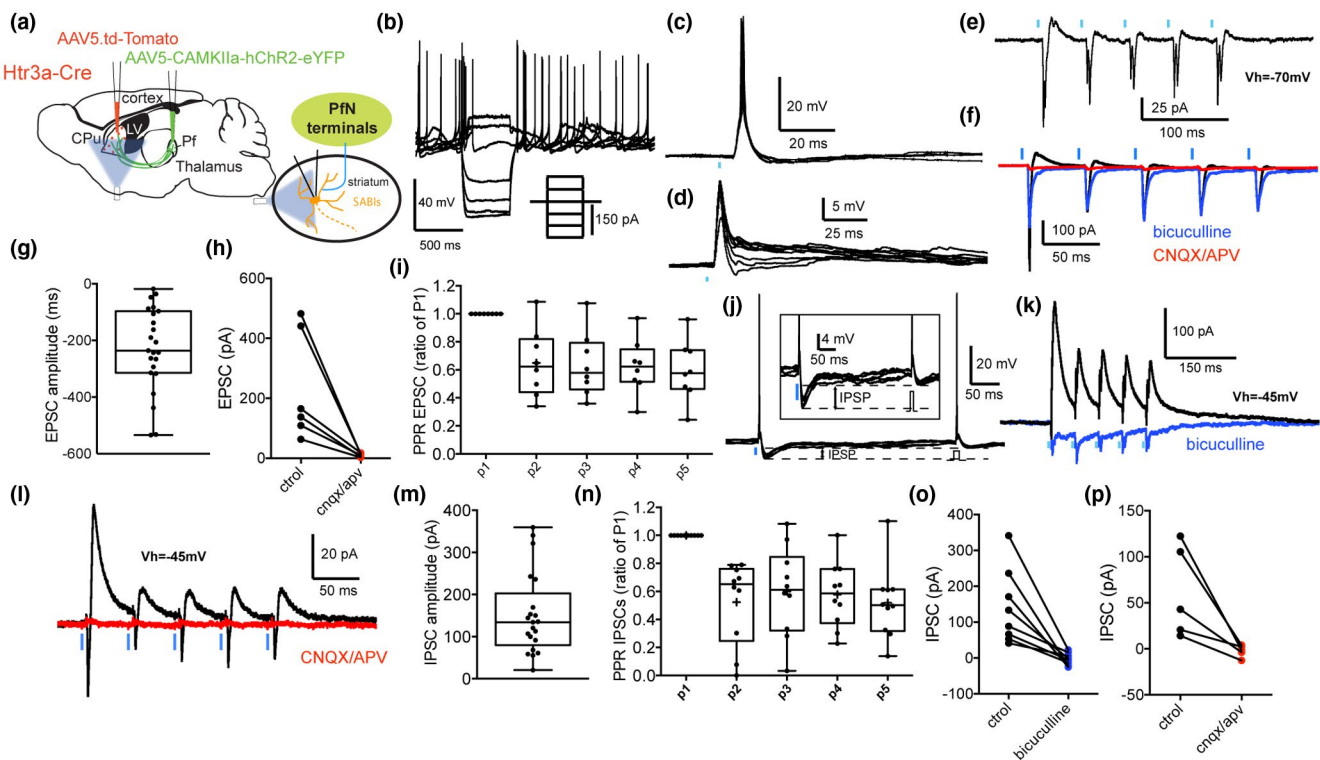
FIGURE 5 Thalamic input to SABIs. (a) Experimental preparation. (b) Typical responses to current injection in a SABI in whole-cell recording. (c) Optogenetic stimulation of thalamostriatal terminals evokes action potential firing in a SABI. (d) Optogenetic stimulation evokes EPSPs. (e) EPSC-IPSC sequence to thalamic train stimulation (5 pulses, 20 Hz, Vh = −70 mV). (f) The IPSC is blocked by a GABA$_A$ receptor antagonist (bicuculline, 10 μM, blue) and the EPSC by glutamate receptor antagonists (CNQX/APV, 10 μM, red, quantified in h; Vh = −70 mV). (g) Box plot quantifying the size of the EPSC. (i) Histograms representing the short-term plasticity of the EPSCs (5 pulses, 20 Hz). (j) Whole-cell current clamp recording of a SABI. Action potentials on the left are induced optogenetically, while action potentials on the right are induced by current injection. Note in inset that the optogenetic stimulation evokes an action potential followed by an IPSP. (k) Optogenetic stimulation also evokes an IPSC (Vh = −45 mV) blocked by bicuculline (10 μM, blue, quantified in o). Train stimulation (5 pulses, 20 Hz) shows that the IPSCs are depressing (quantified in box plots in n). (l) The evoked IPSCs (and EPSCs) can also be blocked by CNQX/APV (10 μM, red, quantified in p). (m) Box plot quantifying the size of the IPSC

not in SABIs. In contrast, optogenetic stimulation of thalamostriatal terminals originating from the PfN evokes distinct disynaptic inhibitory responses in both THINs and SABIs. These results show that both THINs and SABIs participate in polysynaptic (disynaptic) intrastriatal pathways and receive both strong extrinsic monosynaptic excitatory innervation as well as local inhibitory input from as yet unidentified populations of striatal GABAergic interneurons.

4.1 | Extrinsic innervation to the THINs and SABIs

We have previously shown that THINs respond to local or cortical electrical stimulation with monosynaptic glutamatergic EPSPs (Assous & Tepper, 2018; Ibáñez-Sandoval et al., 2010). Here, using optogenetic activation following viral ChR2 transduction (predominantly) in the motor cortex, we confirm the glutamatergic cortical innervation of THINs. Furthermore, we also demonstrate that in about half of the recorded THINs this excitatory response is accompanied by a disynaptic inhibitory synaptic response. Our data suggest that cortical stimulation also activates a population of striatal GABAergic interneurons that innervate THINs. The identity of this GABAergic interneuron(s) is still unknown but could comprise THINs themselves, SABIs, FSIs, LTSIs, or others (such as cell types targeted in the 5HT3a[EGFP] mouse but not in the Htr3a-Cre transgenic (Munoz-Manchado et al., 2016)). Since we also previously demonstrated that SPNs provide a feedback innervation to the THINs (Ibáñez-Sandoval et al., 2010), we cannot rule out the possibility that SPNs could contribute to the disynaptic corticostriatal inhibitory responses in THINs.

The striatum also receives dense innervation from the thalamic PfN (Smith et al., 2014, 2004). Among striatal GABAergic interneurons, FSIs and NGFIs have been shown to receive a strong thalamic innervation (Assous et al., 2017; Rudkin & Sadikot, 1999; Sciamanna et al., 2015; Sidibe & Smith, 1999). Here, we confirm that THINs also receive suprathreshold excitatory thalamic input from the PfN. In a previous study, we showed that thalamic excitation of THINs was responsible for the disynaptic inhibition of LTSIs after optogenetic PfN stimulation (Assous et al., 2017). Here, we demonstrated that ~60% of recorded THINs also exhibit disynaptic IPSC/Ps following stimulation of PfN axon terminals. Similar to cortical-induced IPSCs, we suggest that a population of striatal GABAergic neurons that project to THINs is responsible. However, the cortical- and thalamic-induced IPSCs in THINs exhibit very different short-term plasticities. This suggests that these inhibitory responses may be mediated by different populations of striatal GABAergic neurons. This is consistent with a high level of specificity in the integration of extrinsic glutamatergic input by the striatal circuitry (Assous & Tepper, 2018). One possible scenario is that there is one population of striatal GABAergic interneurons that is selectively activated by the cortex but not the thalamus (LTSIs for example) and another population selectively (or preferentially) activated by thalamic input (e.g., the NGFIs) but that both of them innervate the THINs and thereby

precisely regulate the spike-timing of THINs differentially contingent on the particular excitatory input involved.

The afferent and efferent connections of the SABIs remain largely unknown. These interneurons share many intrinsic electrophysiological properties with THINs including a relatively high input resistance, a depolarization induced inactivation ("depolarization block") in responses to modest depolarizing current injections and the presence of a plateau potential at the end of a positive somatic current injection (Ibáñez-Sandoval et al., 2010). However, SABIs also exhibit some fundamental differences from THINs including their morphology, spontaneous bursting pattern in cell-attached mode, and a lack of synaptic connectivity with SPNs (Assous et al., 2018; Tepper et al., 2018). The latter was the basis for proposing that the SABIs were a type of interneuron-selective interneuron in the mouse striatum (Assous et al., 2018). Here, we demonstrated that SABIs receive monosynaptic innervation from the cortex. In cell-attached recordings, the optogenetic stimulation of corticostriatal terminals induced long bursts of action potentials in the SABIs, similar to spontaneously occurring bursts in these neurons (Assous et al., 2018).

The short-term plasticity of the excitatory response of SABIs is different from that of the cortical input to THINs suggesting the participation of different groups of cells. In contrast to the cortical innervation of THINs, optogenetic stimulation of corticostriatal axons never elicited disynaptic inhibitory responses in SABIs. This indicates that the interneuron responsible for the disynaptic inhibition of THINs after cortical stimulation does not also innervate the SABIs.

In addition, we showed that SABIs are also innervated by thalamostriatal glutamatergic afferents. This input is also functionally powerful as the optogenetic stimulation of thalamostriatal fibers is able to generate action potential firing in SABIs. Similar to thalamic input to the THINs the short-term plasticity of these excitatory responses is depressing, perhaps suggesting innervation by similar group of cells. Interestingly, this stimulation also evokes disynaptic inhibitory responses in the majority of recorded SABIs. Those IPSCs exhibit significantly larger amplitude than the thalamic induced IPSCs in THINs or LTS (albeit these were recorded in different set of animals, Assous et al., 2017). The short-term plasticity of these disynaptic IPSCs in SABIs is depressing which contrasts with the disynaptic IPSCs in THINs. This difference suggests that the interneurons responsible for the disynaptic IPSCs in THINs and SABIs are quite likely different cell types. Here, we can exclude the participation of SPNs in this SABI disynaptic circuit as SPNs do not significantly innervate SABIs (Assous et al., 2018). This highlights once again the very high level of specialization and synaptic selectivity in the striatal circuitry where two different populations of striatal GABAergic interneurons are activated by thalamic afferents and selectively innervate SABIs or THINs. Another nonexclusive possibility is that the IPSCs arise from a combination of different striatal interneurons, or that single populations of striatal interneurons are capable of exhibiting different synaptic plasticities in different target populations.

4.2 | Functional significance

An increasing amount of literature supports an essential role of thalamo- and corticostriatal projections in a multitude of striatal-dependent behavioral functions (Assous et al., 2017; Bradfield, Bertran-Gonzalez, Chieng, & Balleine, 2013; Diaz-Hernandez et al., 2018; Ding et al., 2010; Kupferschmidt, Augustin, Johnson, & Lovinger, 2019; Kupferschmidt, Juczewski, Cui, Johnson, & Lovinger, 2017; Martiros, Burgess, & Graybiel, 2018; Owen, Berke, & Kreitzer, 2018; Smith et al., 2014; Smith, Surmeier, Redgrave, & Kimura, 2011; Tanimura, Du, Kondapalli, Wokosin, & Surmeier, 2019). Some of these effects are attributed to thalamic or cortical innervation of SPNs and others to the innervation of striatal interneurons (see Assous & Tepper, 2018).

Originally, striatal GABAergic interneurons were considered to function mainly as elements of feedforward inhibitory circuits, receiving extrinsic innervation from the cortex and thalamus and modulating spike-timing of the SPNs. However, accumulating evidence suggests that their function in striatal neuronal integration is more complex. As an example, we recently described highly specific interconnection between striatal GABAergic interneurons (i.e., THINs project to LTSIs but not to FSIs or NGFI; Assous et al., 2017) and between cholinergic interneurons and striatal GABAergic interneurons (Assous and Tepper (2018). Furthermore, the SABIs do not significantly synapse onto SPNs and their function is likely to be the inhibition of other striatal interneurons (Assous et al., 2018). In addition, we provided evidence that the extrinsic innervation of striatal interneurons is not uniform but very specific. For instance, LTSIs are not targeted by input from the PfN. In contrast, other GABAergic interneurons seem to be more sensitive to thalamic input than cortical input (e.g., NGFI; Assous et al., 2017). Here, we suggest that selective interneuron–interneuron connections may be specifically engaged by the thalamo- or corticostriatal afferents as shown by the different disynaptic inhibition measured in THINs and SABIs and that these different interneurons, by virtue of their own intrinsic properties (e.g., whether they evoke $GABA_{Afast}$ or $GABA_{Aslow}$ synaptic responses [English et al., 2012; Ibáñez-Sandoval et al., 2010] and/or their homo-or heterosynaptic electrotonic coupling [Tepper & Koós, 2017, Tepper et al., 2018]) are suggested to act in turn to modify the spike-timing and/or synchrony of SPNs, which are a major determinant of activity downstream in the basal ganglia and eventually in the output nuclei.

Therefore, understanding intrastriatal interneuronal connections is fundamental to understand how the different extrinsic inputs to the striatum are processed within the local circuitry and how they will ultimately affect the responses of the projection neurons and downstream basal ganglia circuitry.

DECLARATION OF TRANSPARENCY

The authors, reviewers, and editors affirm that in accordance to the policies set by the Journal of Neuroscience Research, this manuscript presents an accurate and transparent account of the study being reported and that all critical details describing the methods and results are present.

CONFLICT OF INTEREST

None.

AUTHOR CONTRIBUTIONS

Methodology, M.A. and J.M.T.; *Formal Analysis*, M.A.; *Writing— Original Draft*, M.A. and J.M.T.

DATA ACCESSIBILITY

The data that support the findings of this study are available from the corresponding author upon reasonable request.

ORCID

Maxime Assous iD https://orcid.org/0000-0001-6039-816X
James M. Tepper iD https://orcid.org/0000-0002-8643-4082

REFERENCES

Alexander, G. E., DeLong, M. R., & Strick, P. L. (1986). Parallel organization of functionally segregated circuits linking basal ganglia and cortex. *Annual Review of Neuroscience*, *9*, 357–381. https://doi.org/10.1146/annurev.ne.09.030186.002041

Assous, M., Faust, T. W., Assini, R., Shah, F., Sidibe, Y., & Tepper, J. M. (2018). Identification and characterization of a novel spontaneously active bursty GABAergic interneuron in the mouse striatum. *Journal of Neuroscience*, *38*, 5688–5699. https://doi.org/10.1523/JNEUROSCI.3354-17.2018

Assous, M., Kaminer, J., Shah, F., Garg, A., Koós, T., & Tepper, J. M. (2017). Differential processing of thalamic information via distinct striatal interneuron circuits. *Nature Communications*, *8*, 15860. https://doi.org/10.1038/ncomms15860

Assous, M., & Tepper, J. M. (2018). Excitatory extrinsic afferents to striatal interneurons and interactions with striatal microcircuitry. *European Journal of Neuroscience*, *49*, 593–603. https://doi.org/10.1111/ejn.13881

Berendse, H. W., & Groenewegen, H. J. (1990). Organization of the thalamostriatal projections in the rat, with special emphasis on the ventral striatum. *The Journal of Comparative Neurology*, *299*, 187–228. https://doi.org/10.1002/cne.902990206

Bradfield, L. A., Bertran-Gonzalez, J., Chieng, B., & Balleine, B. W. (2013). The thalamostriatal pathway and cholinergic control of goal-directed action: Interlacing new with existing learning in the striatum. *Neuron*, *79*, 153–166. https://doi.org/10.1016/j.neuron.2013.04.039

Buchwald, N. A., Price, D. D., Vernon, L., & Hull, C. D. (1973). Caudate intracellular response to thalamic and cortical inputs. *Experimental Neurology*, *8*, 311–323.

Cruikshank, S. J., Lewis, T. J., & Connors, B. W. (2007). Synaptic basis for intense thalamocortical activation of feedforward inhibitory cells in neocortex. *Nature Neuroscience*, *10*, 462–468. https://doi.org/10.1038/nn1861

Diaz-Hernandez, E., Contreras-Lopez, R., Sanchez-Fuentes, A., Rodriguez-Sibrian, L., Ramirez-Jarquin, J. O., & Tecuapetla, F. (2018). The thalamostriatal projections contribute to the initiation and execution of a sequence of movements. *Neuron*, *100*, 739–752.e5. https://doi.org/10.1016/j.neuron.2018.09.052

Ding, J. B., Guzman, J. N., Peterson, J. D., Goldberg, J. A., & Surmeier, D. J. (2010). Thalamic gating of corticostriatal signaling by cholinergic interneurons. *Neuron*, *67*, 294–307. https://doi.org/10.1016/j.neuron.2010.06.017

Ding, J., Peterson, J. D., & Surmeier, D. J. (2008). Corticostriatal and thalamostriatal synapses have distinctive properties. *Journal of Neuroscience*, *28*, 6483–6492. https://doi.org/10.1523/JNEUROSCI.0435-08.2008

Ellender, T. J., Harwood, J., Kosillo, P., Capogna, M., & Bolam, J. P. (2013). Heterogeneous properties of central lateral and parafascicular thalamic synapses in the striatum. *Journal of Physiology*, *591*, 257–272. https://doi.org/10.1113/jphysiol.2012.245233

English, D. F., Ibáñez-Sandoval, O., Stark, E., Tecuapetla, F., Buzsáki, G., Deisseroth, K., … Koós, T. (2012). GABAergic circuits mediate the reinforcement-related signals of striatal cholinergic interneurons. *Nature Neuroscience*, *15*, 123–130. https://doi.org/10.1038/nn.2984

Faust, T. W., Assous, M., Shah, F., Tepper, J. M., & Koós, T. (2015). Novel fast adapting interneurons mediate cholinergic-induced fast GABAAinhibitory postsynaptic currents in striatal spiny neurons. *European Journal of Neuroscience*, *42*, 1764–1774. https://doi.org/10.1111/ejn.12915. Epub 2015 May 9.

Faust, T. W., Assous, M., Tepper, J. M., & Koós, T. (2016). Neostriatal GABAergic interneurons mediate cholinergic inhibition of spiny projection neurons. *Journal of Neuroscience*, *36*, 9505–9511.

Flaherty, A. W., & Graybiel, A. M. (1993). Output architecture of the primate putamen. *Journal of Neuroscience*, *13*, 3222–3237. https://doi.org/10.1523/JNEUROSCI.13-08-03222.1993

Francois, C., Percheron, G., Parent, A., Sadikot, A. F., Fenelon, G., & Yelnik, J. (1991). Topography of the projection from the central complex of the thalamus to the sensorimotor striatal territory in monkeys. *The Journal of Comparative Neurology*, *305*, 17–34. https://doi.org/10.1002/cne.903050104

Gabernet, L., Jadhav, S. P., Feldman, D. E., Carandini, M., & Scanziani, M. (2005). Somatosensory integration controlled by dynamic thalamocortical feed-forward inhibition. *Neuron*, *48*, 315–327. https://doi.org/10.1016/j.neuron.2005.09.022

Gerfen, C. R., Paletzki, R., & Heintz, N. (2013). GENSAT BAC cre-recombinase driver lines to study the functional organization of cerebral cortical and basal ganglia circuits. *Neuron*, *80*, 1368–1383. https://doi.org/10.1016/j.neuron.2013.10.016

Gittis, A. H., & Kreitzer, A. C. (2012). Striatal microcircuitry and movement disorders. *Trends in Neurosciences*, *35*, 557–564. https://doi.org/10.1016/j.tins.2012.06.008

Haber, S. N. (2016). Corticostriatal circuitry. *Dialogues in Clinical Neuroscience*, *18*, 7–21.

Haber, S. N., Kim, K. S., Mailly, P., & Calzavara, R. (2006). Reward-related cortical inputs define a large striatal region in primates that interface with associative cortical connections, providing a substrate for incentive-based learning. *Journal of Neuroscience*, *26*, 8368–8376. https://doi.org/10.1523/JNEUROSCI.0271-06.2006

Hintiryan, H., Foster, N. N., Bowman, I., Bay, M., Song, M. Y., Gou, L., … Dong, H.-W. (2016). The mouse cortico-striatal projectome. *Nature Neuroscience*, *19*, 1100–1114. https://doi.org/10.1038/nn.4332

Ibáñez-Sandoval, O., Tecuapetla, F., Unal, B., Shah, F., Koós, T., & Tepper, J. M. (2010). Electrophysiological and morphological characteristics and synaptic connectivity of tyrosine hydroxylase-expressing neurons in adult mouse striatum. *Journal of Neuroscience*, *30*, 6999–7016. https://doi.org/10.1523/JNEUROSCI.5996-09.2010

Isaacson, J. S., & Scanziani, M. (2011). How inhibition shapes cortical activity. *Neuron*, *72*, 231–243. https://doi.org/10.1016/j.neuron.2011.09.027

Kemp, J. M., & Powell, T. P. (1971). The termination of fibres from the cerebral cortex and thalamus upon dendritic spines in the caudate nucleus: a study with the Golgi method. *Philosophical Transactions of the Royal Society B: Biological Sciences*, *262*, 429–439.

Koós, T., Tepper, J. M., & Wilson, C. J. (2004). Comparison of IPSCs evoked by spiny and fast-spiking neurons in the neostriatum. *Journal of Neuroscience*, *24*, 7916–7922. https://doi.org/10.1523/JNEUROSCI.2163-04.2004

Kupferschmidt, D. A., Augustin, S. M., Johnson, K. A., & Lovinger, D. M. (2019). Active zone proteins RIM1alphabeta are required for normal corticostriatal transmission and action control. *Journal of Neuroscience*, *39*, 1457–1470.

Kupferschmidt, D. A., Juczewski, K., Cui, G., Johnson, K. A., & Lovinger, D. M. (2017). Parallel, but dissociable, processing in discrete corticostriatal inputs encodes skill learning. *Neuron*, *96*, 476–489.e5. https://doi.org/10.1016/j.neuron.2017.09.040

Mallet, N., Le Moine, C., Charpier, S., & Gonon, F. (2005). Feedforward inhibition of projection neurons by fast-spiking GABA interneurons in the rat striatum in vivo. *Journal of Neuroscience*, *25*, 3857–3869. https://doi.org/10.1523/JNEUROSCI.5027-04.2005

Mandelbaum, G., Taranda, J., Haynes, T. M., Hochbaum, D. R., Huang, K. W., Hyun, M., … Sabatini, B. L. (2019). Distinct cortical-thalamic-striatal circuits through the parafascicular nucleus. *Neuron*, pii: S0896-6273(19)30170-9. https://doi.org/10.1016/j.neuron.2019.02.035 [Epub ahead of print].

Martiros, N., Burgess, A. A., & Graybiel, A. M. (2018). Inversely active striatal projection neurons and interneurons selectively delimit useful behavioral sequences. *Current Biology*, *28*, 560–573.e5. https://doi.org/10.1016/j.cub.2018.01.031

Mathai, A., & Smith, Y. (2011). The corticostriatal and corticosubthalamic pathways: Two entries, one target. So what? *Frontiers in Systems Neuroscience*, *5*, 64. https://doi.org/10.3389/fnsys.2011.00064

McFarland, N. R., & Haber, S. N. (2000). Convergent inputs from thalamic motor nuclei and frontal cortical areas to the dorsal striatum in the primate. *Journal of Neuroscience*, *20*, 3798–3813. https://doi.org/10.1523/JNEUROSCI.20-10-03798.2000

Munoz-Manchado, A. B., Foldi, C., Szydlowski, S., Sjulson, L., Farries, M., Wilson, C., … Hjerling-Leffler, J. (2016). Novel striatal GABAergic interneuron populations labeled in the 5HT3a(EGFP) mouse. *Cerebral Cortex*, *26*, 96–105.

Owen, S. F., Berke, J. D., & Kreitzer, A. C. (2018). Fast-spiking interneurons supply feedforward control of bursting, calcium, and plasticity for efficient learning. *Cell*, *172*, 683–695.e15. https://doi.org/10.1016/j.cell.2018.01.005

Parthasarathy, H. B., & Graybiel, A. M. (1997). Cortically driven immediate-early gene expression reflects modular influence of sensorimotor cortex on identified striatal neurons in the squirrel monkey. *Journal of Neuroscience*, *17*, 2477–2491. https://doi.org/10.1523/JNEUROSCI.17-07-02477.1997

Ramanathan, S., Hanley, J. J., Deniau, J. M., & Bolam, J. P. (2002). Synaptic convergence of motor and somatosensory cortical afferents onto GABAergic interneurons in the rat striatum. *Journal of Neuroscience*, *22*, 8158–8169. https://doi.org/10.1523/JNEUROSCI.22-18-08158.2002

Rudkin, T. M., & Sadikot, A. F. (1999). Thalamic input to parvalbumin-immunoreactive GABAergic interneurons: Organization in normal striatum and effect of neonatal decortication. *Neuroscience*, *88*, 1165–1175. https://doi.org/10.1016/S0306-4522(98)00265-6

Sadikot, A. F., Parent, A., Smith, Y., & Bolam, J. P. (1992). Efferent connections of the centromedian and parafascicular thalamic nuclei in the squirrel monkey: A light and electron microscopic study of the thalamostriatal projection in relation to striatal heterogeneity. *The Journal of Comparative Neurology*, *320*, 228–242. https://doi.org/10.1002/cne.903200207

Sciamanna, G., Ponterio, G., Mandolesi, G., Bonsi, P., & Pisani, A. (2015). Optogenetic stimulation reveals distinct modulatory properties of thalamostriatal vs corticostriatal glutamatergic inputs to fast-spiking interneurons. *Scientific Reports*, *5*, 16742. https://doi.org/10.1038/srep16742

Sidibe, M., & Smith, Y. (1999). Thalamic inputs to striatal interneurons in monkeys: Synaptic organization and co-localization of calcium binding proteins. *Neuroscience*, *89*, 1189–1208. https://doi.org/10.1016/S0306-4522(98)00367-4

Smith, Y., Galvan, A., Ellender, T. J., Doig, N., Villalba, R. M., Huerta-Ocampo, I., ... Bolam, J. P. (2014). The thalamostriatal system in normal and diseased states. *Frontiers in Systems Neuroscience*, *8*, 5. https://doi.org/10.3389/fnsys.2014.00005

Smith, Y., & Parent, A. (1986). Differential connections of caudate nucleus and putamen in the squirrel monkey (Saimiri sciureus). *Neuroscience*, *18*, 347–371. https://doi.org/10.1016/0306-4522(86)90159-4

Smith, Y., Raju, D. V., Pare, J. F., & Sidibe, M. (2004). The thalamostriatal system: A highly specific network of the basal ganglia circuitry. *Trends in Neurosciences*, *27*, 520–527. https://doi.org/10.1016/j.tins.2004.07.004

Smith, Y., Surmeier, D. J., Redgrave, P., & Kimura, M. (2011). Thalamic contributions to basal ganglia-related behavioral switching and reinforcement. *Journal of Neuroscience*, *31*, 16102–16106. https://doi.org/10.1523/JNEUROSCI.4634-11.2011

Tanimura, A., Du, Y., Kondapalli, J., Wokosin, D. L., & Surmeier, D. J. (2019). Cholinergic interneurons amplify thalamostriatal excitation of striatal indirect pathway neurons in Parkinson's disease models. *Neuron*, *101*(3), 444–458.e6. https://doi.org/10.1016/j.neuron.2018.12.004

Tepper, J. M., & Koós, T. (2017). Striatal GABAergic interneurons. In H. Steiner, & K. Y. Tseng (Eds.), *Handbook of basal ganglia structure and function* (2nd ed., pp. 157–178). Cambridge, MA: Academic Press.

Tepper, J. M., Koós, T., Ibanez-Sandoval, O., Tecuapetla, F., Faust, T. W., & Assous, M. (2018). Heterogeneity and diversity of striatal GABAergic interneurons: Update 2018. *Frontiers in Neuroanatomy*, *12*, 91. https://doi.org/10.3389/fnana.2018.00091

Xenias, H. S., Ibanez-Sandoval, O., Koós, T., & Tepper, J. M. (2015). Are striatal tyrosine hydroxylase interneurons dopaminergic? *Journal of Neuroscience*, *35*, 6584–6599. https://doi.org/10.1523/JNEUROSCI.0195-15.2015

Yeterian, E. H., & Van Hoesen, G. W. (1978). Cortico-striate projections in the rhesus monkey: The organization of certain cortico-caudate connections. *Brain Research*, *139*, 43–63. https://doi.org/10.1016/0006-8993(78)90059-8

SUPPORTING INFORMATION

Additional supporting information may be found online in the Supporting Information section at the end of the article. [Correction added on July 30, 2019 after first online publication: The heading 'Transparent Peer Review Report.' was added and Peer review communication document was uploaded online.]

Transparent Science Questionnaire for Authors.

Transparent Peer Review Report.

How to cite this article: Assous M, Tepper JM. Cortical and thalamic inputs exert cell type-specific feedforward inhibition on striatal GABAergic interneurons. *J Neuro Res*. 2019;97:1491–1502. https://doi.org/10.1002/jnr.24444